J Bioenerg Biomembr (2010) 42:151–163
DOI 10.1007/s10863-010-9271-1

Minocycline chelates Ca^{2+}, binds to membranes, and depolarizes mitochondria by formation of Ca^{2+}-dependent ion channels

Yuri N. Antonenko · Tatyana I. Rokitskaya · Arthur J. L. Cooper · Boris F. Krasnikov

Received: 22 December 2009 / Accepted: 3 January 2010 / Published online: 24 February 2010

Abstract Minocycline (an anti-inflammatory drug approved by the FDA) has been reported to be effective in mouse models of amyotrophic lateral sclerosis and Huntington disease. It has been suggested that the beneficial effects of minocycline are related to its ability to influence mitochondrial functioning. We tested the hypothesis that minocycline directly inhibits the Ca^{2+}-induced permeability transition in rat liver mitochondria. Our data show that minocycline does not directly inhibit the mitochondrial permeability transition. However, minocycline has multiple effects on mitochondrial functioning. First, this drug chelates Ca^{2+} ions. Secondly, minocycline, in a Ca^{2+}-dependent manner, binds to mitochondrial membranes. Thirdly, minocycline decreases the proton-motive force by forming ion channels in the inner mitochondrial membrane. Channel formation was confirmed with two bilayer lipid membrane models. We show that minocycline, in the presence of Ca^{2+}, induces selective permeability for small ions. We suggest that the beneficial action of minocycline is related to the Ca^{2+}-dependent partial uncoupling of mitochondria, which indirectly prevents induction of the mitochondrial permeability transition.

Keywords Minocycline · Mitochondria · Permeability transition · Bilayer membrane · Channel formation

Y. N. Antonenko · T. I. Rokitskaya
A.N. Belozersky Institute of Physico-Chemical Biology,
Moscow State University,
Moscow 119992, Russia

A. J. L. Cooper · B. F. Krasnikov (✉)
Department of Biochemistry and Molecular Biology,
New York Medical College,
15 Dana Road, BSB, NYMC,
Valhalla, NY 10595, USA
e-mail: boris_krasnikov@nymc.edu

Introduction

Minocycline (7-dimethylamino-6-dimethyl-6-deoxytetracycline; see Fig. 1) is an FDA approved anti-inflammatory derivative of tetracycline that possesses a number of clinically useful properties. The non-antibiotic properties of this drug have been intensively investigated and have been shown to be beneficial in a number of disparate medical conditions, including rosacea, bullous dermatoses, neutrophilic diseases, pyoderma gangrenosum, sarcoidosis, aortic aneurysms, cancer metastasis, periodontitis, and autoimmune disorders such as rheumatoid arthritis and scleroderma (reviewed in: Sipos et al. 1994; Sapadin and Fleischmajer 2006).

It has been reported that some of the favorable effects of minocycline are related to its ability to influence mitochondrial functioning. For example, Lin et al. (2002) showed that minocycline treatment reduces the levels of RNA transcripts of mitochondrion-encoded genes in the protozoan *Plasmodium falciparum*. Several groups have reported that minocycline prevents, or considerably lowers, pathophysiologically related cytochrome *c* (cyt*C*) release from mitochondria—a key process leading to apoptosis. Work from Friedlander's laboratory showed that minocycline inhibits cyt*C* release in rodent models of amyotrophic lateral sclerosis (Zhu et al. 2002), Huntington disease (Wang et al. 2003) and spinal cord injury (Teng et al. 2004). The authors suggested that the cyt*C* release that was inhibited by minocycline is mediated by the mitochondrial permeability transition (MPT) (Zhu et al. 2002; Wang et al. 2003; Teng et al. 2004). Data presented by Matsuki et al. (2003) indicated that minocycline suppresses heat stress-induced release of cyt*C* from mitochondria both in vitro and in vivo. Scarabelli et al. showed that minocycline significantly reduces the expression level of initiator caspases, increases the ratio of X-linked inhibitor of

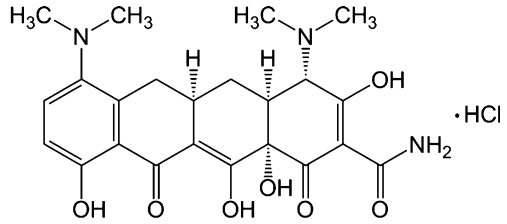

Fig. 1 Structural formula of Minocycline

apoptosis protein to Smac/DIABLO at both the messenger RNA and protein level, and prevents release of cyt*C* and Smac/DIABLO from mitochondria (Scarabelli et al. 2004). It was also reported that under stressful or pathological conditions, minocycline protects mitochondria by inducing up-regulation of antiapoptotic Bcl-2 and down-regulation of proapoptotic Bax, Bak, Bid (Wang et al. 2004; Castanares et al. 2005), and Fas (Chu et al. 2005) proteins. An underlying mechanism for this protection was suggested to result from a decrease in membrane damage and cyt*C* release, leading to blockage of downstream caspase activation (Wang et al. 2004; Castanares et al. 2005; Chu et al. 2005). In these reports (Wang et al. 2004; Castanares et al. 2005; Chu et al. 2005), the authors proposed that the beneficial effects of minocycline involve direct or indirect inhibition of MPT in mitochondria.

However, studies that were performed by Jordán's group on cerebral granular cells using a malonate-induced model of apoptosis showed that minocycline in the concentration range of 10–100 μM is not cytoprotective (Fernandez-Gomez et al. 2005a). The authors presented data indicating that minocycline is not able to prevent Bcl-2 down-regulation by malonate. In the set of experiments conducted by this group on isolated mitochondria, the authors showed that minocycline is protective against Ca^{2+}-induced mitochondrial swelling. The authors suggested that this effect might be mediated through dissipation of the mitochondrial membrane potential ($\Delta\Psi$) and inhibition of Ca^{2+} uptake (Fernandez-Gomez et al. 2005b). Recently, other groups have presented data indicating that the neuroprotective mechanism of minocycline in animals and humans is not related to the inhibition of MPT (Cornet et al. 2004; Mansson et al. 2007). Furthermore, Smith et al. (2003) have suggested that minocycline at high micromolar concentrations might even be toxic rather than protective.

Very recently, Kupsch et al. (2009) suggested that the apparent discrepancy in the effects of minocycline that have been reported by different groups may likely be related to the difference in experimental conditions that were used. The authors showed that in a KCl-based incubation medium, but not in a sucrose-based buffer, minocycline administered directly to the isolated mitochondria triggers mitochondrial swelling and cyt*C* release (Kupsch et al. 2009). The authors also presented data indicating that minocycline, even in low micromolar concentrations in a KCl-based buffer, impairs several energy-dependent functions of mitochondria in vitro such as $\Delta\Psi$ and substrate-dependent oxygen (O_2) uptake (Kupsch et al. 2009). The authors provided strong evidence that the major effects of minocycline on mitochondria are likely related to its ability to deplete endogenous mitochondrial [Mg^{2+}] and induce inner mitochondrial membrane (IMM) permeabilization (Kupsch et al. 2009). The finding that minocycline induces permeabilization of the IMM is undoubtedly an important step forward in the study of this drug. Nevertheless, the question "Is the actual mechanism of such permeabilization related to the MPT or to a phenomenon that is unrelated to the MPT?" still remains to be answered.

It has been shown that some antibiotics of the tetracycline family exhibit ionophoric properties in model membrane systems. For example, chlortetracycline, which has a close structural similarity to minocycline, was shown to transport calcium ions through an organic solvent phase in a pH-dependent manner (White and Pearce 1982). Based on this information, we suggest that minocycline may induce ion fluxes across the IMM. However, there is no evidence in the literature that minocycline directly interacts with mitochondria. The present study was designed to determine whether minocycline directly interacts with mitochondria and possesses channel-forming abilities. To accomplish these goals, experiments were carried out with isolated rat liver mitochondria (RLM), a planar bilayer lipid membrane (BLM) model and a liposome model.

Materials and methods

Chemicals

β-Alanine, micro Biuret protein assay kit, bovine serum albumin (fatty acid free grade Sigma A-6003), $CaCl_2$, EGTA, gramicidin A, Hepes (ultra grade), minocycline, KCl, KOH, KH_2PO_4, MES, Ruthenium 360 (Ru360), succinate, sucrose (ultra grade), PBS-Tween buffer, and Tris-base were obtained from Sigma (St. Louis, MO, USA). Cholesterol, dioleoylphosphatidylcholine, dioleoylphosphatidylglycerol, 1,2-diphytanoyl-*sn*-glycero-3-phosphocholine, diphytanoyl-phosphatidylcholine (DPhPC), egg phosphatidylcholine and *Escherichia coli* total lipid fraction were obtained from Avanti Polar Lipids (Alabaster, AL, USA). *n*-Decane was obtained from Merck (Darmstadt, Germany). All reagents used were of the highest purity available.

Recordings of minocycline spectra

Minocycline was dissolved in ethanol and then diluted with water to yield a final concentration of 20 mM in 10%

ethanol. Minocycline is unstable in solution if stored at room temperature; when the solution is stored in the refrigerator (4 °C), it is stable for not more than two weeks. Therefore, minocycline solutions were used no later than one week after preparation and storage at 4 °C. Minocycline spectra were recorded in a plate reader SpectraMax 340 system (Molecular Devices Corporation, Downingtown, PA, USA) using untreated, medium binding, Corning 96-well clear flat bottom polystyrene plates (Thomas Scientific Inc., Swedesboro, NJ, USA).

Isolation of rat liver mitochondria and mitochondrial experiments

Mitochondria were isolated from six-month old male/female Fisher 344X Brown Norway F_1 rats (fed *ad libitum* and with full access to water) by the procedure described previously (Krasnikov et al. 2005). All procedures were carried out on ice in a 4 °C cold room. Mitochondria isolated using this procedure and kept on ice were stable (as judged by consistent ADP/O ratio and RCR values) for at least 12 h after isolation. The mitochondrial protein concentration was determined by the micro Biuret method.

Mitochondrial functioning was assessed by using a multi-parameter chamber (for details see Krasnikov et al. 2005), which permits simultaneous measurement of four mitochondrial parameters: O_2 uptake using a Clark-type closed electrode; calcium ion flux by means of a Ca^{2+}-selective electrode and a reference electrode; $\Delta\Psi$ using a TPP^+-selective electrode and reference electrode; swelling as reflected by changes in transmittance at 660 nm (by means of a light-emitting and a photo diodes).

The experimental incubation buffer consisted of 300 mM sucrose, 5 mM Hepes, 2.5 mM KH_2PO_4 supplemented with 5 mM succinate and 1 μM rotenone, pH adjusted to 7.4 with Tris-base. The concentrations of the reagents added to the mitochondria in all experiments presented here were such that the volume (1 ml) was altered by less than 2%. All additions listed in the figure legends are final concentrations.

Experimental design for determination of minocycline binding to mitochondria

RLM protein concentration was varied from 0.25 to 3 mg/ml. Minocycline was used at concentrations of 100 and 200 μM. The concentration of Ca^{2+} was varied from 5 μM to 2 mM. Mitochondria were incubated with minocycline in 1 ml of sucrose buffer (300 mM sucrose, 3 mM Hepes, 2.5 mM KH_2PO_4, 5 mM succinate plus 1 μM rotenone, pH 7.4) on ice for either 3 or 5 min (except where noted). Controls were identical except that minocycline was omitted. After incubation, the mitochondria were centrifuged at 14,000 *g* for 10 min at 4 °C. The supernatant was carefully removed, labeled as the 'Super' fraction and saved. The mitochondrial pellet was re-suspended in 1 ml of PBS-Tween buffer (10 mM phosphate-buffered saline, 0.5% (v/v) Tween, pH 7.4). The procedure results in solubilization of most of the mitochondrial pellet. The solubilized sample was centrifuged at 14,000 *g* for 10 min at 4 °C. The supernatant was removed, labeled as the 'Pellet' fraction and saved. A very small amount of insoluble material was discarded.

The 'Super' fraction contained minocycline unbound to RLM, whereas the 'Pellet' contained minocycline bound to mitochondria. In order to obtain the spectrum of minocycline in the 'Pellet' fraction it was necessary to subtract the blank spectrum due to detergent and mitochondrial components in the sample.

We investigated the possibility of using a filtration procedure to rapidly separate suspension buffer from mitochondria. However, we found that variable amounts (up to 30%) of minocycline were bound to the filter membranes (data not shown). Therefore, in all experiments carried out on mitochondria, the incubation buffer was removed by centrifugation.

Planar bilayer lipid membranes

To verify the suggestion that minocycline can induce conductivity in phospholipid membranes, a set of experiments was carried out using the planar BLM model. BLMs were formed from a 2% solutions of DPhPC, 1,2-diphytanoyl-sn-glycero-3-phosphocholine or *E. coli* total lipid extract in *n*-decane by the brush technique (Mueller et al. 1963). Lipid was applied to a 0.55-mm diameter hole in a Teflon partition that separates two compartments of a specially designed cell (see Mueller et al. 1963 for details). Both compartments were filled with buffer containing 100 mM KCl, 10 mM MES, 10 mM Tris, 10 mM β-alanine, pH 8.5 (unless otherwise stated). The electrical current (I) was measured with an amplifier (Keithley 428, Keithley Instruments, Cleveland, OH, USA), digitized by a LabPC 1200 (National Instruments, Austin, TX, USA), and analyzed using WinWCP Strathclyde Electrophysiology Software designed by J. Dempster (University of Strathclyde, UK). A voltage of 60 mV (unless otherwise stated) was applied to the BLM with Ag/AgCl electrodes placed directly into the cell.

Detection of proton transport in pyranine-loaded liposomes

The lumenal pH of the liposomes was assayed with pyranine [a fluorescent dye with a $pK_a \sim 7.3$ and a λ_{ex}= 405 nm in its acid form (−3 charge) and a λ_{ex}=455 nm in its basic form (−4 charge)] by a slight modification of the previously published procedure (Chen et al. 1999). Briefly, to prepare pyranine-loaded liposomes, lipids (5 mg of egg

phosphatidylcholine and 1 mg of cholesterol) in a chloroform suspension were dried in a round bottom flask under a stream of nitrogen. The lipids were then resuspended in buffer (100 mM KCl, 20 mM MES, 20 mM MOPS, 20 mM Tricine titrated with KOH to pH 6.0) containing 0.5 mM pyranine. The suspension was vortexed and then freeze-thawed 3 times. Unilamellar liposomes were prepared by extrusion through 0.1-μm-pore size Nucleopore polycarbonate membranes using an Avanti Mini-Extruder. The unbound pyranine was then removed by passage through a Sephadex G-50 coarse column equilibrated with the same buffer solution. Pyranine leakage from the liposomes was less than 1% per day. The liposomes were used within 1 week of preparation. To measure the rate of pH dissipation in liposomes with a lumenal pH 6.0, the liposomes were diluted in a solution buffered to pH 8.0. The emission fluorescence at 510 nm (excitation 455 nm) was monitored with a Panorama Fluorat 02 spectrofluorimeter (Lumex, Russia). At the end of each recording, 1 μM nigericin was added to dissipate the remaining pH gradient.

Leakage assay with carboxyfluorescein-loaded liposomes

Liposomes were prepared from the same lipid mixture as described in the above section in a solution containing 100 mM carboxyfluorescein titrated with Tris-base to pH 8.5. The unloaded carboxyfluorescein was then removed by passage through a Sephadex G-50 coarse column using an eluting buffer containing: 100 mM KCl, 20 mM MES, 20 mM MOPS, and 20 mM Tricine titrated with KOH to pH 8.0. To measure the rate of carboxyfluorescein leakage, the liposomes were diluted in the same buffer. The emitted fluorescence was monitored at 520 nm (excitation 490 nm) as described above. At the end of each recording, 1 μM mellitin was added to complete the leakage process.

All experiments were carried out at room temperature (~20 °C) unless indicated otherwise. All results presented here are average ± standard deviation and were calculated using SigmaPlot 2000 software; *p* values were calculated by the paired *t*-test using Microsoft Excel software.

Results

Determination of an isosbestic point in the minocycline spectrum that is independent of buffer composition, pH and [Ca^{2+}]

The minocycline spectrum was noted to change in the presence of Ca^{2+}, indicating formation of complex(es) between these two components (Fig. 2, A Panels). In this respect, it should be emphasized that correct measurement of minocycline concentrations must take into account possible alterations in the spectrum of the compound in different buffers and under different conditions. To this end, measurement of minocycline concentrations should be determined at the wavelength of an isosbestic point. For the sucrose buffer, the Ca^{2+}-independent minocycline isosbestic point was found to be at ~358 nm (Fig. 2, B Panels).

Due to the fact that mitochondrial experiments were carried out with different buffers (Hepes, Sucrose, and PBS*Tween) it was also necessary to determine the Ca^{2+}-independent isosbestic points for minocycline in all the buffers used (Fig. 2, C Panels). We also took into account the possibility that a potential change in pH may occur during the mitochondrial experiments. Therefore, isosbestic points for different pH and Ca^{2+} values were obtained (Fig. 2, D Panels). Finally, we found that the Ca^{2+}-, buffer-, and pH-independent isosbestic points for minocycline were in a very close range of ~356–360 nm. Thus, under conditions in which Ca^{2+} or pH might change unpredictably, the concentration of the total minocycline can still be calculated from the absorbance at the isosbestic point (~358 nm).

In order to calculate the amount of the complex formed between minocycline and Ca^{2+} (Mino*Ca) the concentration dependence of the free minocycline (Mino) at 340 nm absorbance (peak of the minocycline spectrum; Fig. 3, Panel A) was first determined, and an equation and coefficients of the linear regression were established (Fig. 3, Panel B). Next, a series of titrations with increasing Ca^{2+} concentrations (0–100 μM) was performed using a single 100 μM concentration of minocycline. The decrease in absorbance at 340 nm corresponded to an increase in the Ca^{2+}-related formation of the Mino*Ca complex (Fig. 3, Panel C). The values of the absorbance for each [Ca^{2+}] at 340 nm were used to calculate the concentration of Mino using the equation and coefficients of the linear regression shown in Panel B. Mino*Ca was calculated as 100 μM minus Mino. Titration of minocycline (100 μM) over the range of 0 to 2 mM Ca^{2+} was performed. The dependence of the Mino*Ca/Mino ratio on [Ca^{2+}] is presented in Fig. 3, Panels D and E. Panel D shows Ca^{2+}-dependent (sigmoidal) changes in the Mino*Ca/Mino ratio over a wide range of Ca^{2+} concentrations in sucrose buffer. Panel E of Fig. 3 shows the linear ratio dependence at low concentrations of Ca^{2+} (0–200 μM). The concentration of Ca^{2+} required to yield a Mino*Ca/Mino ratio equal to 1 was determined from the linear regression plot shown in Panel E. This value is the Ca^{2+}-binding constant K_{Ca2+} for the Mino*Ca complex and is ~65 μM (see the "Discussion").

Binding of minocycline to mitochondria

RLM at a total protein concentration of 1 mg/ml were incubated in sucrose buffer containing 200 μM minocycline for 5 min on ice. After incubation the samples were

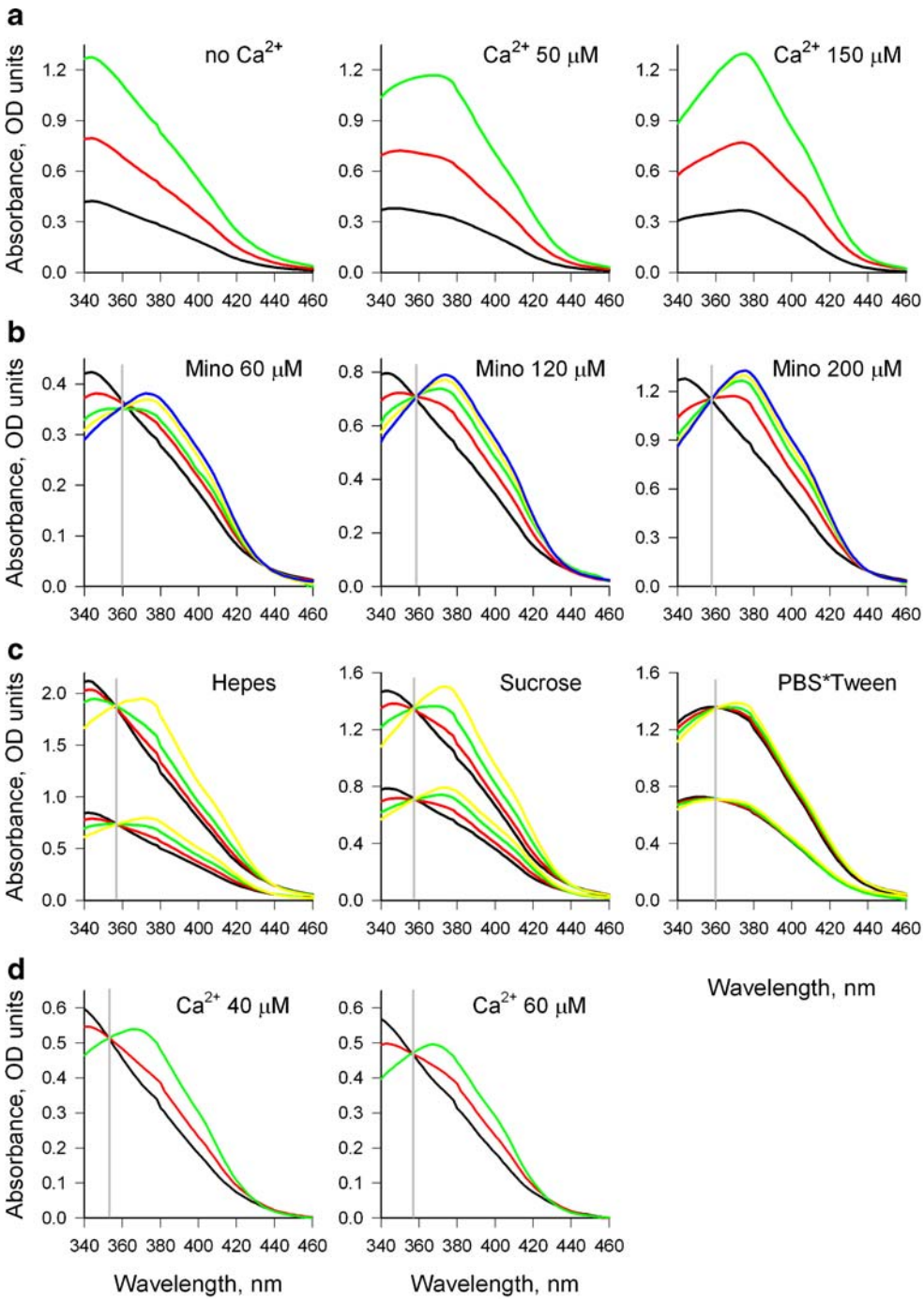

Fig. 2 Determination of isosbestic points for the minocycline spectrum under different experimental conditions. (**A** Panels) Ca^{2+}-dependent changes in the spectrum of minocycline at three different concentrations (Black, 60 μM; Red, 120 μM; Green, 200 μM) in sucrose buffer at three different [Ca^{2+}]. (**B** Panels) Determination of the Ca^{2+}-independent isosbestic points for minocycline spectra in sucrose buffer at three concentrations of minocycline (Mino) at four [Ca^{2+}] (Black, no Ca^{2+}; Red, 50 μM; Green, 100 μM; Yellow, 150 μM; Blue, 200 μM). (**C** Panels) Dependence of the minocycline spectra on the experimental buffer and [Ca^{2+}]. The Hepes buffer contained 3 mM Hepes, pH 7.4; the Sucrose buffer consisted of 300 mM sucrose, 3 mM Hepes, pH 7.4; and the PBS*Tween buffer contained 10 mM phosphate-buffered saline, 0.5 % Tween, pH 7.4. The minocycline concentration was 100 and 200 μM ([Ca^{2+}]: Black, no Ca^{2+}; Red, 20 μM; Green, 50 μM; Yellow, 100 μM). (**D** Panels) pH dependence (Black, pH 6.6; Red, pH 7.4; Green, pH 8.2) of the minocycline (80 μM) spectrum in sucrose buffer supplemented with 40 and 60 μM Ca^{2+}

centrifuged at 14,000 *g* and the spectrum of minocycline in the supernatant was recorded. The concentration of minocycline was calculated from the absorbance at the isosbestic point (~358 nm). The minocycline concentrations in the control buffer (lacking mitochondria), and two experimental supernatants (RLM, no Ca^{2+} added; and RLM, 50 μM Ca^{2+} added) were: 200, 132±16.5 and 78±10.5 μM, respectively (Fig. 4, Panel A).

The mitochondria-induced decrease in minocycline concentration in the supernatant suggests that this compound binds to these organelles. The Ca^{2+}-induced increase in minocycline binding to RLM was investigated. The concentrations of RLM and minocycline were fixed at 1 mg/ml and 100 μM, respectively, but the concentration of Ca^{2+} was varied from 0 to 100 μM. After incubation in sucrose buffer on ice for 3 min, the amount of minocycline bound to RLM was determined from the concentration of the minocycline remaining in the supernatant, and is presented as nmol/mg of mitochondrial protein (Fig. 4, Panel B). From the data depicted in this figure, one can

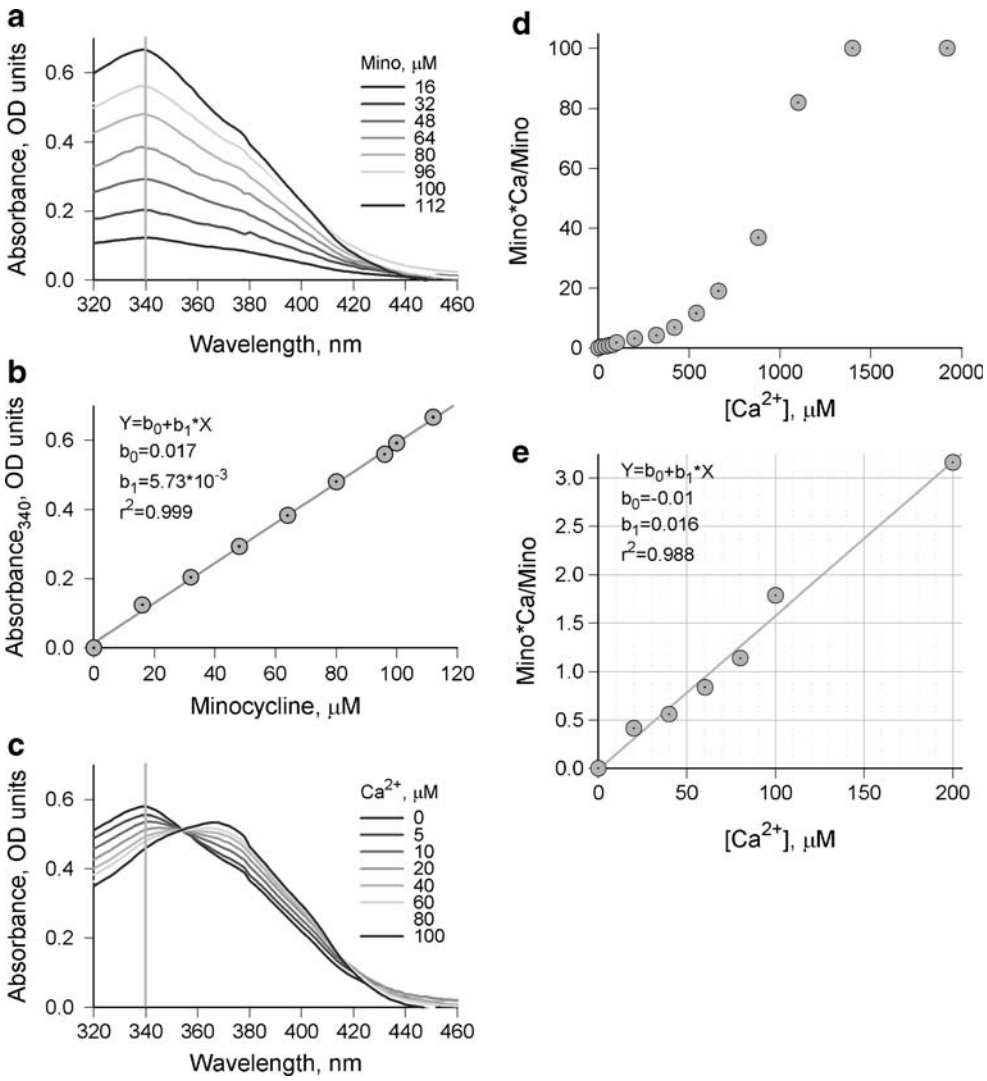

Fig. 3 Calculation of the ratio of the complex formed between minocycline and Ca^{2+} (Mino*Ca) to free minocycline (Mino) in sucrose buffer. (Panel **A)** Concentration dependence of the minocycline (Mino) spectra. (Panel **B)** Calibration curve for Mino absorbance at 340 nm versus concentration, showing the equation and coefficients of the linear regression. (Panel **C)** Ca^{2+}-dependent changes in the spectrum of 100 μM minocycline. The values of the absorbance for each Ca^{2+} concentration at 340 nm in Panel C were used to calculate the concentration of Mino using the equation of the linear regression from Panel B. [Mino*Ca] was calculated as 100 μM minus [Mino]. (Panel **D**) The sigmoidal dependence of the Mino*Ca/Mino ratio over a wide range of $[Ca^{2+}]$. (Panel **E)** Linearity of Mino*Ca/Mino versus $[Ca^{2+}]$ in the low $[Ca^{2+}]$ range of Panel D. The binding constant (K_{Ca2+}) found from Panel E for Ca^{2+} in the presence of 100 μM minocycline is ~65 μM as determined from the value of the Mino*Ca/Mino ratio equal to 1

calculate that the maximal amount of minocycline bound to RLM is ~60 nmol/mg of protein. Maximal binding requires the presence of at least 40 μM Ca^{2+}.

The time dependence for minocycline binding to mitochondria was determined in sucrose buffer under the following conditions: 0.5 mg/ml RLM was incubated on ice for 3 min with 100 μM minocycline, followed by an additional period of incubation in the presence or absence of 50 μM Ca^{2+} (Fig. 5, Panel A). The $T_{1/2}$ value for minocycline binding in the presence of Ca^{2+} was shorter (less than 1.5 min) compared to that obtained in the absence of Ca^{2+} (~2.5 min).

The dependence of minocycline (200 μM) binding on the concentration of mitochondria was also investigated. Binding was determined after 5 min incubation on ice in a reaction mixture in which the final volume was 1 ml (Fig. 5, Panel B). Minocycline binding was found to be satisfactorily described by the following empirical equation: $Y = a(1 - b^x)$. This equation holds true whether or not Ca^{2+} (50 μM) was present in the buffer. In both cases, regression analysis yielded r^2 coefficients of 0.991. The equation predicts a maximum amount of minocycline bound to mitochondria (corresponding to 3 mg of protein) of 170 nmol. Half of the minocycline binding occurred with mitochondrial amounts corresponding to ~0.5 mg and ~1.8 mg of protein, respectively, in the presence and absence of Ca^{2+} (Fig. 5, Panel B).

Effect of minocycline on mitochondrial ion fluxes

The effect of minocycline on Ca^{2+}-induced MPT in RLM was investigated using the multiparameter chamber (Krasnikov et al. 2005). Four parameters were measured simultaneously in the same sample: O_2 uptake, Ca^{2+} flux, $\Delta\Psi$ and swelling. Representative results are shown in Fig. 6. The experimental conditions were: sucrose buffer, RLM 0.45 mg/ml, additions: Ca^{2+} = 60 μM, minocycline = 100 μM and Ru360 = 100 μg/ml (Ru360 is a specific inhibitor of the mitochondrial Ca^{2+} uniporter (Matlib et al. 1998)).

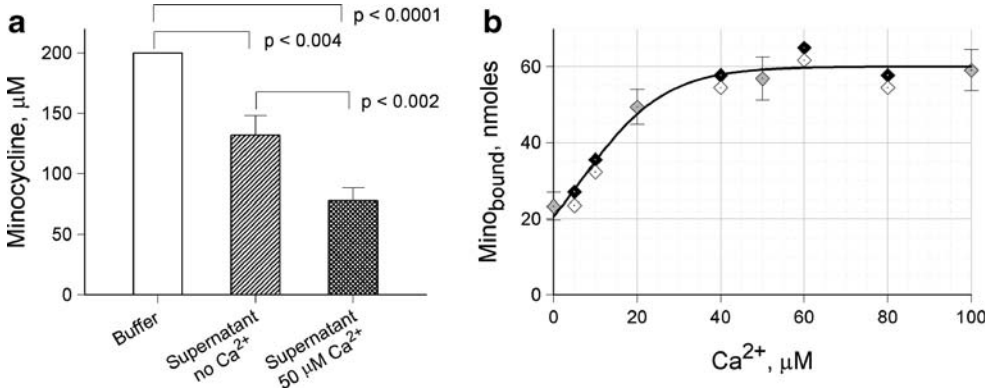

Fig. 4 (Panel **A**) Decrease of minocycline (200 μM) concentration in sucrose buffer (1 ml) after incubation with RLM (1 mg/ml) for 5 min on ice in the absence or presence of 50 μM Ca^{2+}. *N*=4. (Panel **B**) Ca^{2+}-dependence of minocycline (100 μM) binding to mitochondria (1 mg/ml/3min). Gray diamond symbols with error bars are the average ± standard deviation. *N*=4. White and black diamond symbols represent values from two experiments. The sucrose buffer contained 300 mM sucrose, 3 mM Hepes, 2.5 mM KH_2PO_4, and 5 mM succinate plus 1 μM rotenone, pH 7.4

The classical Ca^{2+}-induced MPT in RLM is characterized by: 1) a nonlinear increase of O_2 uptake, 2) an initial sequestration of added Ca^{2+} followed by its release, 3) an initial drop of ΔΨ followed by recovery and further dissipation, and 4) a high-amplitude swelling (e.g. Krasnikov et al. 2005). See also Fig. 6, Panels A–D, traces 'a'.

Addition of 60 μM Ca^{2+} to RLM previously incubated with Ru360 for 3 min, resulted in 1) no increase in O_2 uptake, 2) no uptake of added Ca^{2+} (the steady state level of Ca^{2+} remained at ~60 μM), 3) no dissipation of ΔΨ, and 4) no swelling (Fig. 6, Panels A–D, traces 'c').

We found that the initial addition of minocycline to RLM caused 1) a linear increase in O_2 uptake, 2) a significant drop, followed by partial recovery of ΔΨ, and 3) a short (less than 1 min), but rapid, initial decrease in absorbance, followed by a plateau (Fig. 6, Panels A–D, traces 'b').

Addition of Ca^{2+} in the presence of minocycline did not affect the linear increase in O_2 uptake. No uptake of added Ca^{2+} was recorded (Fig. 6, Panel A, trace 'b'), and the steady state level of the Ca^{2+} remained at ~30–35 μM (Fig. 6, Panel B, trace 'b'). At the time at which Ca^{2+} was added, the ΔΨ was completely abolished (Fig. 6, Panel C, trace 'b'), and a short (~2 min), rapid decrease in absorbance occurred, followed by a trend toward a plateau (Fig. 6, Panel D, trace 'b').

We found that in the KCl-based buffer (KCl 150 mM), the minocycline-related decrease in ΔΨ was somewhat stronger and the rate of this decrease was more rapid compared to the relatively slow dissipation of ΔΨ that occurred in sucrose buffer (Fig. 7, Panel A). At pH 8.0 addition of minocycline almost completely abolished ΔΨ, whereas at pH 6.8 the change in ΔΨ was similar to that which occurred at neutral pH (Fig. 7, Panel C). In contrast to the sucrose buffer where addition of Ca^{2+} completely abolished ΔΨ, partial restoration of the potential was observed after addition of Ca^{2+} in KCl-based buffer (Fig. 7, Panel A). The level of ΔΨ restoration was dependent on KCl concentration (data not shown).

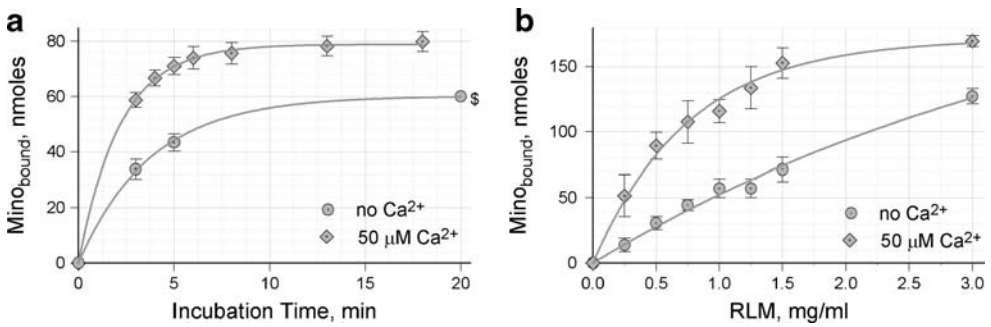

Fig. 5 (Panel **A**) Time-dependence of minocycline (100 μM) binding to RLM (0.5 mg of protein/ml). *N*=4. (Panel **B**) Minocycline (200 μM) binding (5 min on ice) to RLM is dependent on RLM concentration and the presence of Ca^{2+}. The values are the average ± standard deviation. *N*=4, except for a single measurement indicated as '$'. Individual sets of experiments in Panels A and B were carried out four months apart, which may have introduced some variability. The experimental buffer conditions were the same as those described in the legend to Fig. 2 and the total volume of the experimental mixture was 1 ml

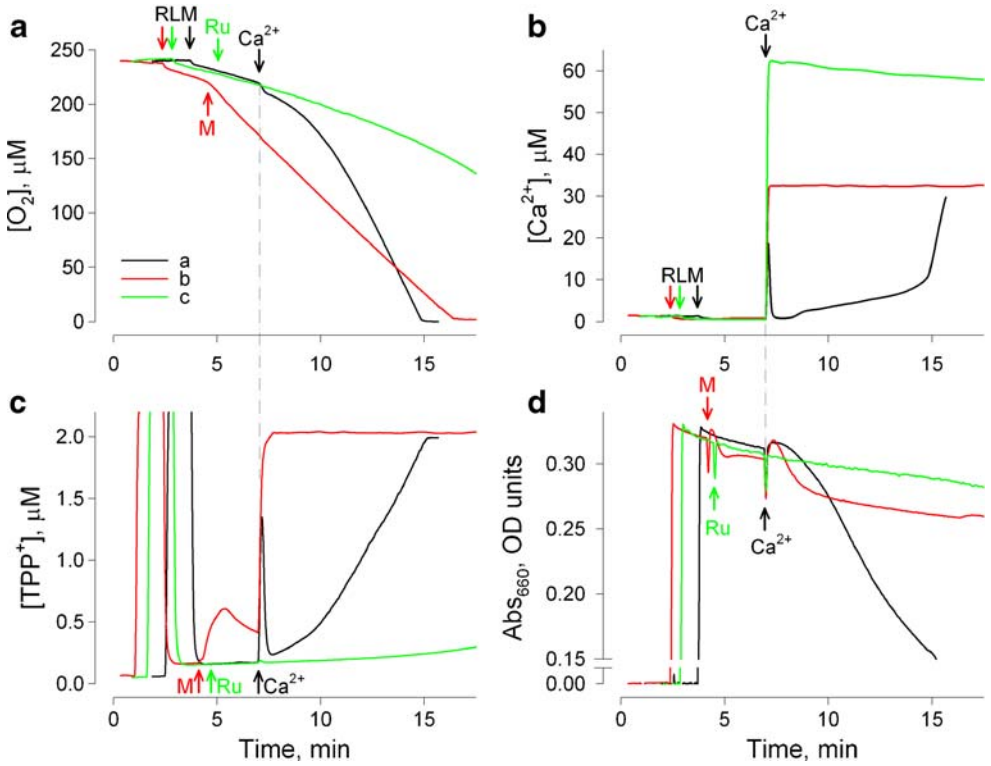

Fig. 6 Effects of different treatments on four parameters measured simultaneously in RLM. Traces 'a', MPT induction by Ca^{2+}; traces 'b', effect of minocycline; traces 'c', inhibitory effect of Ru360 on MPT. Experimental conditions: sucrose buffer contained 300 mM sucrose, 3 mM Hepes, 2.5 mM KH_2PO_4, and 5 mM succinate plus 1 μM rotenone, pH 7.4. The RLM concentration was 0.45 mg/ml. Additions of Ca^{2+}, minocycline (M) and Ru360 (Ru) were 60, 100 μM and 100 μg/ml, respectively. Panels **A**–**D**: O_2 uptake, Ca^{2+} flux, ΔΨ, and swelling, respectively. (Panel **A**) The decrease in O_2 concentration reflects O_2 uptake by mitochondria. (Panel **B**) The increase in Ca^{2+} concentration indicates either Ca^{2+} efflux from mitochondria or absence of Ca^{2+} influx into mitochondria. (Panel **C**) The increase in TPP^+ concentration reflects ΔΨ dissipation. (Panel **D**) The decrease in absorbance indicates mitochondrial swelling. The traces are representative of at least four experiments obtained with different mitochondrial preparations

With regard to the inhibition of Ca^{2+}-induced mitochondrial swelling in KCl-based buffer, minocycline induced short-term low-amplitude initial swelling followed by a steady-state. Addition of Ca^{2+} did not cause swelling, but rather a slight shrinkage of mitochondria compared to that in sucrose-based buffer (Fig. 7, Panel B). The inhibitory effect of minocycline on mitochondrial swelling was greater at pH 8.0 compared to that at pH 6.8 (Fig. 7, Panel D). Panels A and B in Fig. 7 indicate that the initial effects of minocycline on ΔΨ and swelling are much more pronounced in 150 mM KCl compared to those in sucrose buffer. Panels C and D in Fig. 7 also show that the effects of minocycline on these parameters are greater under slightly basic compared to slightly acidic conditions in sucrose buffer.

To obtain further insights into the mechanism by which minocycline affects mitochondria functioning, experiments were performed on model membranes.

Minocycline induces anion permeability in planar BLM

To test the possibility that minocycline induces ion permeability in BLM the electrical current was measured in this model system. A typical trace of the increase in the current upon the addition of minocycline in the presence of Ca^{2+} is shown in Fig. 8, Panel A. The increase in the noise during 23–27 min was a result of stirring of the solutions. The experiment was performed at alkaline pH (8.5) because the effect at pH 7.0 was much less pronounced. It is important to note that neither minocycline nor Ca^{2+} alone was effective in the induction of the electrical current under these conditions (data not shown).

The data presented in Panel A of Fig. 8 are more consistent with ion channel activity than with carrier-mediated conductance. To emphasize this point the experiments were carried out at higher sensitivity and lower conductance. A typical trace of minocycline-mediated current under single-channel conditions is shown in Panel B of Fig. 8. The predominant channel conductance was calculated to be 14 pS at 1 M KCl. These data were obtained at a high concentration of Ca^{2+} (3 mM), which is comparable to total calcium that may be present inside the mitochondrial matrix under normal physiological conditions. However, it should be noted that the channel activity can be observed even at relatively low calcium concentration (i.e. 20 μM, Fig. 8, Panel C).

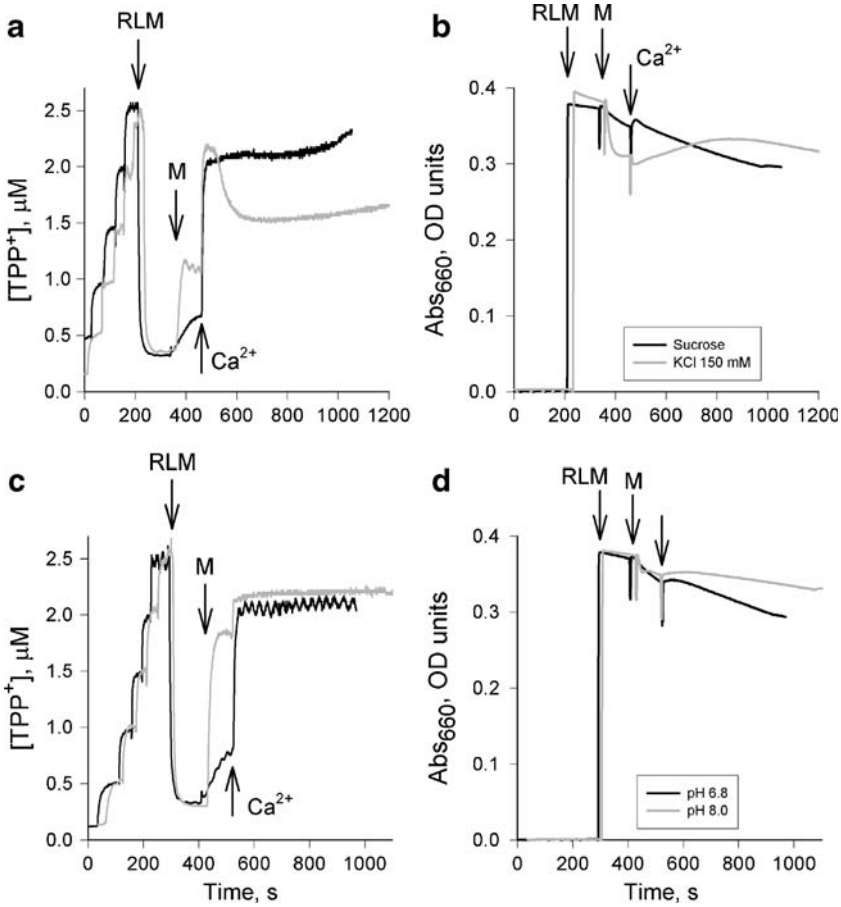

Fig. 7 Effects of minocycline on ΔΨ and swelling of mitochondria upon addition of Ca^{2+}. (Panels **A** and **B**) Sucrose- (black traces) and 150 mM KCl buffer (gray traces), respectively. (Panels **C** and **D**) The effects of minocycline on ΔΨ and swelling of RLM under slightly acidic (pH 6.8, black traces) and slightly basic (pH 8.0, gray traces) conditions in Sucrose buffer, respectively. Additions: RLM, rat liver mitochondria 0.5 mg/ml; M, minocycline 200 μM; Ca^{2+} 60 μM (enough to induce the MPT-trace not shown)

The concentration-dependence of the minocycline-mediated current is shown in Panel A of Fig. 9. The dependence was strongly nonlinear, indicating that the number of molecules forming the channel varies with concentration. To determine the ion selectivity of minocycline-mediated channels, I-V curves were measured under symmetrical (Fig. 9, Panel B, closed circles) and asymmetrical conditions (Fig. 9, Panel B, open circles). The value of zero-voltage current under asymmetrical conditions (12 mV; with the "plus" sign at the side with higher KCl concentration) corresponds to the ratio of chloride anion to potassium cation permeability, which according to the Goldman-Hodgkin-Katz equation was estimated to be about 9.

The voltage-dependence of the minocycline-mediated ion channel activity (minocycline-mediated membrane conductance) is illustrated in Fig. 10. The conductance increased several times when voltage was increased from

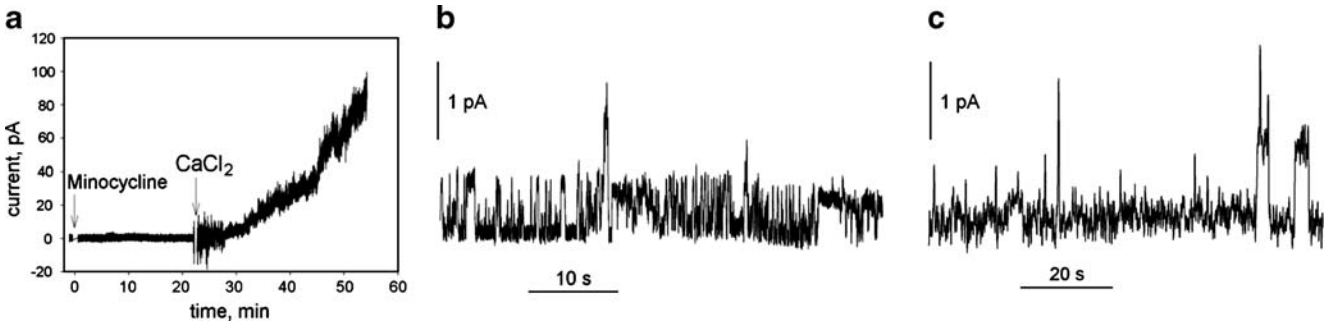

Fig. 8 (Panel **A**) Minocycline (20 μM) in the presence of 3 mM Ca^{2+} induces an electrical current in BLM made from DPhPC. The experimental buffer was 10 mM Tris, 10 mM MES, 100 mM KCl, pH 8.5; the voltage was 30 mV. (Panels **B**, **C**) Ion channel activity induced by minocycline (8 μM) in the presence of Ca^{2+} (3 mM in panel B and 20 μM in panel C) at 50 mV in BLM made from DPhPC. The experimental buffer was 10 mM Tris, 10 mM MES, 1 M KCl, pH 9.0. (A current of 0.7 pA at 50 mV corresponds to a conductance of 14 pS)

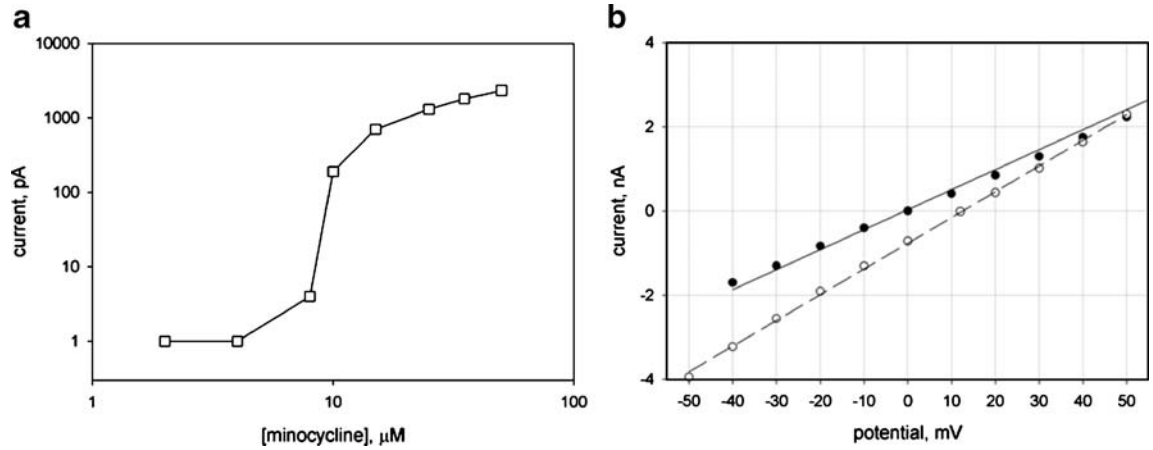

Fig. 9 (Panel **A**) The dependence of the BLM electrical current on the concentration of minocycline at V=50 mV. (Panel **B**) I-V curves for minocycline (50 μM)-mediated electrical current under symmetrical (100 mM:100 mM KCl; closed circles) and asymmetrical (190 mM:100 mM KCl; open circles) conditions. BLM was made from DPhPC in the presence of Ca^{2+} (3 mM). The experimental buffer conditions were the same as described for Fig. 8, Panel A

+50 to +150 mV, suggesting formation of additional channels at high voltages. It is important to note that the dependence of the channel activity on the applied voltage in the range from +50 to +150 mV was completely reversible (data not shown).

Minocycline induces proton permeability in liposomes

After establishing that minocycline forms channels in planar BLM, it was important to determine next whether such channels are capable of conducting protons, because normal mitochondrial functioning requires maintenance of a proton gradient. To investigate this possibility, a more sensitive model than the planar BLM model was employed. Lipid vesicles with entrapped pyranine are a very sensitive system for measurement of proton fluxes at pH values of ~7.0 (Chen et al. 1999). The kinetics of pyranine fluorescence after the addition of minocycline in the presence and absence of 5 mM $CaCl_2$ are shown in Panel A of Fig. 11. Liposomes with a mildly acidic interior (pH 6.0) were placed in a medium buffered at pH 8.0. The increase in fluorescence after the addition of minocycline indicates acceleration of proton equilibration, i.e. induction of proton permeability. Minocycline was ineffective in the absence of Ca^{2+} (Fig. 11, Panel A, gray curve). As a control, addition of nigericin was used to abolish the pH gradient.

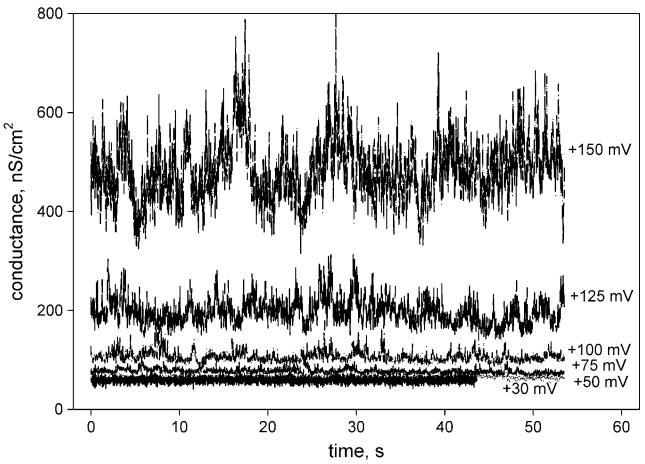

Fig. 10 Dependence of the BLM conductance on the voltage applied in the presence of 20 μM minocycline and 3 mM $CaCl_2$. The BLM was made from an *E. coli* total lipid fraction. The experimental buffer conditions were the same as those described for Fig. 8, Panel A

It was also important to be sure that minocycline induces proton permeability without affecting the integrity of the liposomal membranes. To verify this point, a model system consisting of liposomes loaded with carboxyfluorescein was used. This methodology has higher sensitivity compared to that described above for the measurements of proton fluxes. No leakage of carboxyfluorescein was detected in this model either in the presence of minocycline alone or in the presence of minocycline plus Ca^{2+} (Fig. 11, Panel B). This result indicates that the ion channels formed by minocycline are impermeable to carboxyfluorescein. The antibiotic mellitin, which forms channels (~3 nm) in phospholipid membranes (Yang et al. 2001), was used as a control to induce carboxyfluorescein egress. This observation is also consistent with the relatively small size of ion channels formed by minocycline measured electrophysiologically (see above).

Discussion

The data obtained with the planar BLM and liposome models suggest that a combination of minocycline with Ca^{2+} leads to

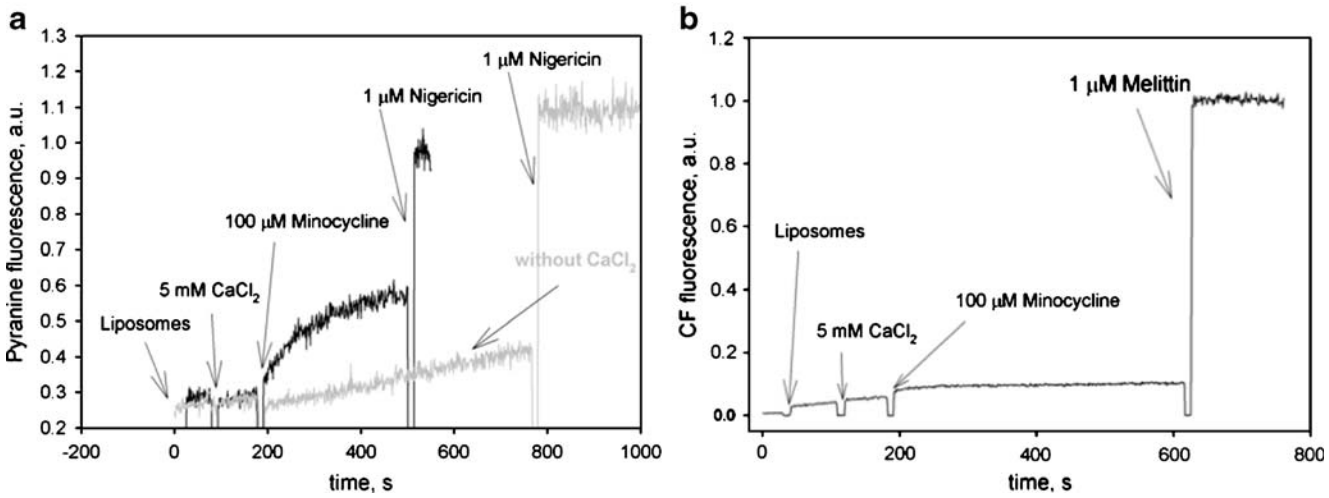

Fig. 11 (Panel **A**) Minocycline induces proton permeability in liposomes loaded with pyranine in the presence of Ca^{2+} (5 mM). Addition of nigericin was used as a positive control. The lipid concentration was 20 μg/ml. Excitation, 455 nm; emission, 505 nm. (Panel **B**) Minocycline does not induce carboxyfluorescein (CF) leakage from dye-loaded liposomes in the presence or absence of Ca^{2+} (5 mM). Addition of melittin was used as a positive control. The lipid concentration was 5 μg/ml. Excitation, 488 nm; emission, 520 nm; a.u., arbitrary units

formation of channels for anions and protons. The pH dependence of this process suggests that the deprotonated form of minocycline is involved in formation of this complex. [This conclusion is also supported by the data obtained with RLM under slightly alkaline (pH 8.0) conditions (Fig. 7, Panel D, gray curve).] Even though the exact mechanism of the channel formation is not yet clear, our work shows that this mechanism is different from the carrier-type of ion transport, which is known for some derivatives of tetracycline (White and Pearce 1982). Based on our findings, we hypothesize that minocycline-derived channel formation in BLM is similar to that of the aminocoumarin antibiotic novobiocin. This drug has been shown to form ion channels in both natural (O'Brodovich et al. 1993) and artificial (Feigin et al. 1995) membranes via its oligomerization. No ions are apparently required for formation of these channels. We suggest that minocycline may also form channels by oligomerization. We wish to emphasize that if this is the case, then unlike novobiocin, the process of channel formation with minocycline strongly requires the presence of Ca^{2+}.

The data discussed in the previous paragraph together with those obtained with RLM suggest that the induction of proton conductance in the mitochondrial membrane is likely the mechanism that underlies mitochondrial depolarization and increased O_2 uptake by RLM in the presence of minocycline (Fig. 6, Panels A,C). The depolarization was substantially increased after the addition of Ca^{2+}, but the rate of O_2 uptake did not change. The data obtained in a KCl-based buffer (Fig. 7, Panel A, gray curve) also suggest that minocycline alone administered to RLM is capable of partial mitochondrial depolarization, which is in accord with the recently reported findings of Kupsch et al. (2009). The combined results on $\Delta\Psi$ and O_2 uptake by mitochondria suggest a phenomenon similar to mild uncoupling.

Addition of Ca^{2+} (final concentration 60 μM) to RLM in the presence of minocycline resulted in a rapidly established steady-state level of Ca^{2+} in the incubation buffer of ~30–35 μM (Fig. 6, Panel B, trace 'b'). However, in the presence of Ru360, addition of Ca^{2+} (final concentration 60 μM) resulted in a Ca^{2+} steady state that was maintained in the range of ~60 μM (Fig. 6, Panel B, trace 'c'). The difference in the steady-state concentration of Ca^{2+} in the presence of minocycline and Ru360 cannot be explained by inhibition of the mitochondrial Ca^{2+} uniporter by minocycline for at least two reasons.

First, we found that minocycline acts as a weak Ca^{2+} chelator with an apparent binding constant of ~65 μM Ca^{2+} (at 100 μM of minocycline, Fig. 3, Panel E). However, at Ca^{2+} concentrations greater than 200 μM, the response deviates from linearity and becomes sigmoidal (Fig. 3, Panel D). This finding suggests formation of Ca^{2+}-minocycline complexes at ratios of ~1:2, 1:1, and 2:1. The formation of even weaker complexes at higher ratios is suggested by the sigmoidal shape of the curve in the presence of saturating Ca^{2+}, but the strongest interaction corresponds to a Mino*Ca/Mino ratio of 1 and occurred at ~65 μM. Formation of the Ca^{2+}-minocycline complex(es) explains the steady-state levels of ~60 μM Ca^{2+} in the presence of Ru360, but only ~30 μM Ca^{2+} in the presence of minocycline, despite the addition of equal amounts of Ca^{2+} to the incubation medium in both experiments (Fig. 6, Panel B, 'b' and 'c' traces, respectively).

Secondly, no change in $\Delta\Psi$ was noted in the presence of Ru360 and Ca^{2+} (Fig. 6, Panel C, trace 'c'). However, a complete collapse of $\Delta\Psi$ occurred when only both

minocycline and Ca^{2+} were added sequentially in sucrose- (Fig. 6, Panel C, trace 'b') or KCl-based buffers (Fig. 7, Panel A). This phenomenon does not take place if only one of the compounds is employed. It is well known that Ca^{2+} flux through its uniporter is dependent on $\Delta\Psi$ (Scott et al. 1980; Gunter and Pfeiffer 1990). Once the $\Delta\Psi$ drops below a certain critical level the uniporter shuts down and Ca^{2+} influx is no longer possible. Ru360 directly and irreversibly blocks the Ca^{2+} uniporter. Therefore, in the presence of this inhibitor, Ca^{2+} influx is prevented, but at the same time $\Delta\Psi$ remains unaffected. On the other hand, our data show that addition of Ca^{2+} causes complete dissipation of $\Delta\Psi$ only in the presence of minocycline, which, in turn, results in transition of the Ca^{2+} uniporter from an open to a closed state.

The minocycline inhibition of RLM swelling can be interpreted, at first glance, erroneously as inhibition of the Ca^{2+}-induced MPT (Fig. 6, Panel D, traces 'a' and 'b'). However, three other parameters that we measured simultaneously (O_2 uptake, $\Delta\Psi$, and Ca^{2+} fluxes) indicate that the effect of minocycline on mitochondria is much more complicated than can be described by a direct MPT inhibition. Our combined data suggest that minocycline prevents Ca^{2+} influx into mitochondria through the following chain of sequential events: partial chelation of Ca^{2+} → incorporation of minocycline-Ca^{2+} complex(es) into mitochondrial membranes → formation of proton and anion selective channels → dissipation of $\Delta\Psi$. It is a well accepted point of view that $\Delta\Psi$, matrix pH and matrix Ca^{2+} play key roles in the MPT induction (Petronilli et al. 1993). Therefore, if prior to addition of Ca^{2+}, mitochondria were depolarized (not necessarily even completely, but just enough to close the Ca^{2+} uniporter), then calcium accumulation will be prevented, and, thus MPT opening will not occur (unless a much higher [Ca^{2+}] is employed (Halestrap et al. 1997)).

Many research groups have studied the effects of minocycline on isolated mitochondria and on cells in culture at concentrations up to 100–200 μM (Zhu et al. 2002; Smith et al. 2003; Wang et al. 2003; Matsuki et al. 2003; Cornet et al. 2004; Teng et al. 2004; Fernandez-Gomez et al. 2005a, b; Mansson et al. 2007; Kupsch et al. 2009). Similarly, we used 100–200 μM concentrations in our studies, which were designed to understand the effect of minocycline on isolated mitochondria. Although 100 μM concentrations of minocycline might be difficult to attain in vivo, our work may nevertheless be of clinical relevance. For example, Kupsch et al. (2009) estimated that pharmacological doses of minocycline used in clinical trials on ALS patients resulted in levels in the brain calculated to be about 20 μM. We noted the ability of minocycline to form channels in artificial bilayers even at concentration as low as 8 μM (Fig. 8, Panel C).

As we stated in the Introduction, the purpose of the present study was to determine whether minocycline directly interacts with mitochondria and possesses channel-forming abilities. The possibility was also considered that minocycline may affect the properties of plasma membranes. To investigate this possibility in detail would require a major separate study. However, a few points can be made indicating that minocycline is unlikely to have a major effect on plasma membrane properties. First, there are many reports in the literature indicating that minocycline easily permeates the blood-brain barrier (Zhu et al. 2002; Wang et al. 2003; Smith et al. 2003; Teng et al. 2004; Cornet et al. 2004; Chu et al. 2005; Sapadin and Fleischmajer 2006; Mansson et al. 2007). Secondly, we performed a set of experiments using an erythrocyte hemolysis model, indicating that under normal physiological conditions minocycline has no major impact on erythrocyte plasma membranes (data not shown).

Thus, in conclusion, we have provided evidence that mitochondria are the primary target for minocycline. Moreover, the effect of minocycline on mitochondria is likely not related to direct inhibition of the Ca^{2+}-induced MPT, but is related to its ability first, to chelate Ca^{2+}, secondly to bind to RLM membranes, thirdly, to partially uncouple mitochondria by formation of ion channels, and, finally, to prevent Ca^{2+} accumulation in the mitochondrial matrix.

Acknowledgements We thank Dr. Bruce S. Kristal for help and encouragement. The project was supported in part by grants from NIH/NIEHS 5RO1 NS38471 and the Russian Fund for Basic Research # 09-04-00890.

References

Castanares M, Vera Y, Erkkila K, Kyttanen S, Lue Y, Dunkel L, Wang C, Swerdloff RS, Hikim AP (2005) Biochem Biophys Res Commun 337:663–669

Chen Y, Schindler M, Simon SM (1999) J Biol Chem 274:18364–18373

Chu HC, Lin YL, Sytwu HK, Lin SH, Liao CL, Chao YC (2005) Br J Pharmacol 144:275–282

Cornet S, Spinnewyn B, Delaflotte S, Charnet C, Roubert V, Favre C, Hider H, Chabrier PE, Auguet M (2004) Eur J Pharmacol 505:111–119

Feigin AM, Aronov EV, Teeter JH, Brand JG (1995) Biochim Biophys Acta 1234:43–51

Fernandez-Gomez FJ, Gomez-Lazaro M, Pastor D, Calvo S, Aguirre N, Galindo MF, Jordán J (2005a) Neurobiol Dis 20:384–391

Fernandez-Gomez FJ, Galindo MF, Gomez-Lazaro M, González-García C, Ceña V, Aguirre N, Jordán J (2005b) Neuroscience 133:959–967

Gunter TE, Pfeiffer DR (1990) Am J Physiol 258:C755–786

Halestrap AP, Woodfield KY, Connern CP (1997) J Biol Chem 272:3346–3354

Krasnikov BF, Zorov DB, Antonenko YN, Zaspa AA, Kulikov IV, Kristal BS, Cooper AJL, Brown AM (2005) Biochim Biophys Acta 1708:375–392

Kupsch K, Hertel S, Kreutzmann P, Wolf G, Wallesch CW, Siemen D, Schönfeld P (2009) FEBS J 276:1729–1738
Lin Q, Katakura K, Suzuki M (2002) FEBS Lett 515:71–74
Mansson R, Hansson MJ, Morota S, Uchino H, Ekdahl CT, Elmer E (2007) Neurobiol Dis 25:198–205
Matlib MA, Zhou Z, Knight S, Ahmed S, Choi KM, Krause-Bauer J, Phillips R, Altschuld R, Katsube Y, Sperelakis N, Bers DM (1998) J Biol Chem 273:10223–10231
Matsuki S, Iuchi Y, Ikeda Y, Sasagawa I, Tomita Y, Fujii J (2003) Biochem Biophys Res Commun 312:843–849
Mueller P, Rudin DO, Tien HT, Wescott WC (1963) J Phys Chem 67:534–535
O'Brodovich H, Wang X, Li C, Rafii B, Correa J, Bear C (1993) Am J Physiol 264:C1532–1537
Petronilli V, Cola C, Bernardi P (1993) J Biol Chem 268:1011–1016
Sapadin AN, Fleischmajer R (2006) J Am Acad Dermatol 54:258–265
Scarabelli TM, Stephanou A, Pasini E, Gitti G, Townsend P, Lawrence K, Chen-Scarabelli C, Saravolatz L, Latchman D, Knight R, Gardin J (2004) J Am Coll Cardiol 43:865–874
Scott ID, Akerman KE, Nicholls DG (1980) Biochem J 192:873–880
Sipos EP, Tamargo RJ, Weingart JD, Brem H (1994) Ann NY Acad Sci 732:263–272
Smith DL, Woodman B, Mahal A, Sathasivam K, Ghazi-Noori S, Lowden PA, Bates GP, Hockly E (2003) Ann Neurol 54:186–196
Teng YD, Choi H, Onario RC, Zhu S, Desilets FC, Lan S, Woodard EJ, Snyder EY, Eichler ME, Friedlander RM (2004) Proc Natl Acad Sci USA 101:3071–3076
Wang X, Zhu S, Drozda M, Zhang W, Stavrovskaya IG, Cattaneo E, Ferrante RJ, Kristal BS, Friedlander RM (2003) Proc Natl Acad Sci USA 100:10483–10487
Wang J, Wei Q, Wang CY, Hill WD, Hess DC, Dong Z (2004) J Biol Chem 279:19948–19954
White JR, Pearce FL (1982) Biochemistry 21:6309–6312
Yang L, Harroun TA, Weiss TM, Ding L, Huang HW (2001) Biophys J 81:1475–1485
Zhu S, Stavrovskaya IG, Drozda M, Kim BY, Ona V, Li M, Sarang S, Liu AS, Hartley DM, Wu DC, Gullans S, Ferrante RJ, Przedborski S, Kristal BS, Friedlander RM (2002) Nature 417:74–78